Tetraalkylammonium Manganese Oxide Gels: Preparation, Structure, and Ion-Exchange Properties

Stephanie L. Brock,[†,⊥] Maria Sanabria,[‡] Jaya Nair,[†] Steven L. Suib,*[,†,‡,§] and Thorsten Ressler[||]

Department of Chemistry, University of Connecticut, 55 North Eagleville Road, Storrs, Connecticut 06269-3060, Department of Chemical Engineering and Institute of Materials Science, University of Connecticut, Storrs, Connecticut 06269, and Fritz-Haber-Institut der MPG, Institut für Anorganische Chemie, Faradayweg 4-6, D-14195 Berlin, Germany

Received: October 25, 2000; In Final Form: March 30, 2001

The structure and ion-exchange properties of tetraalkylammonium (TAA; alkyl = methyl, ethyl, propyl) manganese oxide gels produced from colloidal manganese oxide solutions are presented. TAA manganese oxide xerogels are analyzed by X-ray powder diffraction (XRD) and extended X-ray absorption fine spectra (EXAFS) and can be modeled on an octahedral layered, pseudohexagonal structure. Ion-exchange reactions are performed with Na^+, Mg^{2+}, Ni^{2+}, Cu^{2+}, or La^{3+} with wet gels and the factors that influence the resulting structure and uptake are described. Exchange of xerogels was accomplished only in the presence of base. Despite variations in the sorption of different ions, the TAA cations are completely and rapidly removed from the structure.

Introduction

Porous manganese oxides are a unique class of materials that combine the high surface area/selectivity properties of zeolites with the redox capacity of manganese. As such, they have great potential as selective heterogeneous catalysts, sorbents, and battery materials.[1,2] Porous manganates are either amorphous or else crystallize as tunnel-structured materials (octahedral molecular sieves, OMSs) or layered materials (octahedral layered phases, OLs) and some representative structures are presented in Figure 1. These materials are most commonly prepared using precipitation and/or hydrothermal techniques conducted at relatively low temperature (<250 °C).[2−11] Although structurally similar materials can be prepared by a variety of routes, the physical properties (acid/base, redox, sorption capacity), stability, and catalytic activity are highly dependent on synthetic conditions. Thus, considerable effort has focused on controlling conditions in order to prepare new materials with specific functionality and characteristics.

Sol−gel reactions provide a versatile tool set for the preparation of materials with novel, designed properties.[12] Although extensively investigated for the formation of unique silaceous materials (large zeolite crystals, aerogels, glasses, etc.) the sol−gel chemistry of other metal oxide systems is, by comparison, poorly developed. Only in the past decade have researchers investigated the potential for sol−gel reactions to produce unique manganese oxide materials, despite the fact that the original recipe for manganese oxide "jellies" has been known since the early 20th century.[13,14]

Reactions between permanganate salts and fumaric acid, simple sugars, or poly-ols to yield amorphous gels have been reported.[15−20] These manganese oxide gels can be thermally transformed into porous oxides such as the 2 × 2 octahedra lined tunnel material, OMS-2, and the layered birnessites (OL). Sol−gel processed manganese oxides generally show increased thermal stability relative to conventional preparations[15] and can be made with a high degree of preferred orientation.[21] Furthermore, the electrochemical properties of sol−gel derived OL materials suggest they may be useful as electrodes for battery applications.[21,22]

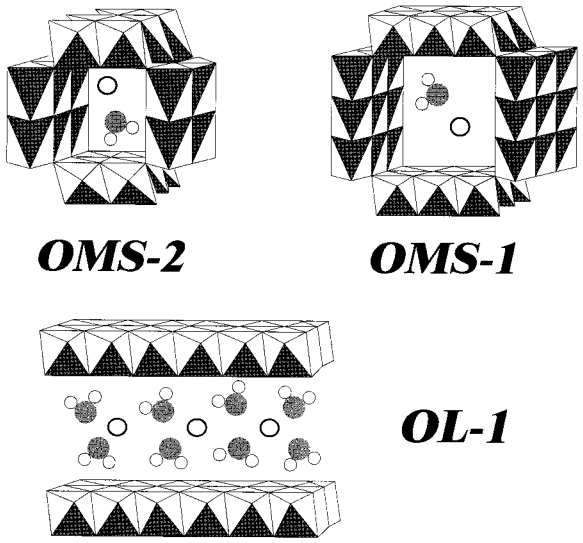

Figure 1. Structures of representative octahedral molecular sieve (OMS) and octahedral layered (OL) phases of manganese oxides. Open circles represent tunnel or interlayer cations, water molecules are indicated by the combination of shaded and open circles.

Recently, we reported a new sol−gel methodology based on the reaction of tetraalkylammonium (TAA) permanganate salts with aqueous 2-butanol solutions.[23] Unlike other systems, a stable colloid of manganese oxide can be formed even at high

* Author to whom correspondence should be addressed.
† Department of Chemistry, University of Connecticut.
‡ Department of Chemical Engineering, University of Connecticut.
§ Institute of Materials Science, University of Connecticut.
|| Fritz-Haber-Institut der MPG, Institut für Anorganische Chemie.
⊥ Current Address: Department of Chemistry, Wayne State University, Detroit, MI 48202.

10.1021/jp003943r CCC: $20.00
Published on Web 05/18/2001

manganese concentrations (up to 0.2 M) and the sol state can be maintained indefinitely. Controlled gelation can be achieved by varying parameters such as aging temperature, TAA cation, and alcohol content. This ability to exert a high degree of control over the gelation process has resulted in some unusual materials, including helical manganese oxide wires.[24] In this paper we describe the properties of generic manganese oxide gels produced from tetramethylammonium (TMA), tetraethylammonium (TEA), and tetrapropylammonium (TPA) colloidal manganese oxide precursors, and compare them to gels produced in other systems and conventionally prepared manganese oxides. The materials reported here are unique in demonstrating a rapid ion exchange with high capacity for metal ions, a high degree of crystallinity, and a reversible sol−gel transition.

Experimental Section

Preparation of Gels. The preparation of tetraalkylammonium (alkyl = methyl, ethyl, propyl) manganese oxide colloids from reduction of tetraalkylammonium (TAA) permanganate in water/2-butanol solutions has been described in detail elsewhere.[23] The colloids are aqueous and consist of anionically charged manganese oxide, TAA cations, and up to 20% 2-butanol by volume. Gels were produced from 0.1 M tetramethylammonium (TMA), tetraethylammonium (TEA), and tetrapropylammonium (TPA) manganese oxide colloids by heating them in sealed polybottles at 85 °C from 1 h to 3 days. The subsequent gels were washed several times with distilled deionized water (DDW) using centrifugation and filtration. Formation of xerogels was achieved by drying the gels at room temperature or at 65 °C. Xerogels could be resuspended by dissolution in 1 M TEAOH or TPAOH aqueous solutions, yielding a reddish-brown colloid. Note: Unlike unsaturated alkylammonium permanganate salts, the salts used here (TMA, TEA, TPA permanganate) do not decompose explosively.[23]

Ion Exchange. A volume of 75 mL of 0.1 M aqueous exchange solutions was combined with a wet, unwashed tetramethylammonium manganese oxide gel (gel volume 75 mL, concentration 0.1 M Mn, room-temperature aging for 6 months), stirred for 1 h, washed several times with centrifugation, and the process repeated with another aliquot. The exchange properties were investigated using sodium chloride (Baker and Adamson), nickel(II) acetate tetrahydrate (Aldrich), copper(II) acetate monohydrate (Johnson Matthey), magnesium acetate tetrahydrate (Janssen), or chloride hexahydrate (Baker), and lanthanum trichloride (Spex). Exchanged gels were dried at room temperature.

Ion-exchange reactions were also carried out with dried gels. Fifty milligrams of TEA manganese oxide xerogel was combined with ~4 mL of 0.1 M NaOH or 5.5 M NaCl and left at room temperature for one week. The xerogels were then filtered and washed several times with DDW.

X-ray Diffraction Studies. A Scintag XDS-2000 diffractometer utilizing Cu Kα radiation was used to obtain diffraction patterns on manganese oxide gels. Xerogels were gently crushed or ground to a powder, and wet gels and colloids were prepared by spreading a thin layer onto a glass slide followed by air-drying.

Thermal Analyses. Thermal gravimetric analyses were performed on xerogels in a nitrogen atmosphere using a TA Instruments TGA 2950. The temperature ramp rate was either 10 °C or 20 °C per minute. Tetraalkylammonium-containing xerogels are extremely combustible and a larger, 100 μL ceramic pan was used to minimize weight loss from the sample being blown out of the pan. To prepare bulk samples for XRD characterization, samples were placed in ceramic crucibles and heated in air in a furnace at temperatures of 100 or 200 °C for 5 h.

Average Oxidation State Titration. The total manganese content of TPA, TEA, and TMA manganese oxide xerogels was determined by dissolution in concentrated hydrochloric acid and titration of Mn^{2+} to Mn^{3+} in sodium pyrosulfate solution using potassium permanganate.[25] On the basis of the total amount of manganese present, the average oxidation state of manganese was determined by reduction of the gel to Mn^{2+} with ferrous ammonium sulfate and back-titration of the excess iron with potassium permanganate.[25]

Chemical Analysis. C,H,N combustion analysis was performed on all samples to determine quantities of tetraalkylammonium cation and 2-butanol present in dried gels and exchanged dried gels. Analyses of Mn, Cu, Ni, La, Na, and Mg were performed using inductively coupled plasma atomic emission spectroscopy with a Perkin-Elmer model P40 spectrometer on acid-digested samples of the dried gels and/or energy-dispersive X-ray analysis (EDAX) in conjunction with scanning electron microscopy.

Scanning Electron Microscopy (SEM). An Amray model 1810 D SEM at a beam voltage of 15−25 kV was used for determination of xerogel morphology. Samples were prepared by grinding the xerogel and sprinkling a small portion of the resultant powder onto a sample holder coated with carbon paste.

Infrared Studies (IR). A Nicolet Magna-IR 750 spectrometer with a DTGS KBr or MCT/B detector was used for IR studies. Samples were prepared either as a KBr pellet for transmittance or placed in a stainless steel cup for diffuse reflectance measurements. KBr samples were prepared by grinding a small amount of sample with dried KBr (Fischer, IR grade) and pressing to 15 000 psi in a pellet press. IR data were obtained from 450 to 4000 cm^{-1}.

X-ray Absorption Spectroscopy Measurements (XAS). XAS experiments were performed on the 31-pole-wiggler beam line 10-2[26] at Stanford Synchrotron Radiation Laboratory (SSRL) with the storage ring operating at an energy of 3.0 GeV and injection current of ~100 mA. A Si(220) double-crystal monochromator was used and higher harmonics in the synchrotron beam were suppressed by detuning the monochromator to ~50% of the maximum of the rocking curve. Samples were prepared as a thin powder layer on Kapton tape ($\Delta\mu = 0.7$) and transmission spectra were recorded at room temperature in a photon energy range from 6.5 to 7.5 keV.

X-ray absorption fine structure (XAFS) analysis was carried out using the software package WinXAS97 v1.2[27] following recommended procedures from the literature.[28] Pre-edge background subtraction and normalization was performed by fitting linear polynomials to the pre-edge and the post-edge region of an absorption spectrum, respectively. A smooth atomic background, $\mu_0(k)$, was obtained using a cubic spline refinement procedure. The radial distribution function FT($\chi(k)$) was obtained by Fourier transforming the k^3-weighted experimental extended fine structure (EXAFS) $\chi(k)$, multiplied by a Bessel window, into R space.

Calculation of theoretical EXAFS spectra and refinement to experimental data was carried out using theoretical backscattering phases and amplitudes obtained from the ab initio multiple-scattering code FEFF 7.[29] EXAFS refinements reported in this work were carried out in R space to magnitude and imaginary part of a Fourier transformed k^3-weighted experimental $\chi(k)$. Further details on the EXAFS refinement procedure employed can be obtained from the cited literature.[30,31]

TABLE 1: Chemical Formula, Manganese Average Oxidation State, and Interlayer Spacing (based on (001) reflections) for TAA Manganese Oxide Xerogels and Na-OL-1 (sodium birnessite)[35]

chemical formula[a]	average oxidation state of Mn	interlayer spacing (Å)
$(TPA)_{0.4}Mn_{14}O_{24.6}\cdot 6.9H_2O$	3.49	12.0
$(TEA)_{2.5}Mn_{14}O_{26.8}\cdot 3.7H_2O$	3.79	17.1
$(TMA)_{2.2}Mn_{14}O_{26.2}\cdot 9.5H_2O$	3.73	9.2
$Na_{4.0}Mn_{14}O_{27.0}\cdot 9.0H_2O$	3.57	7.1

[a] Oxygen content calculated from average oxidation state, formulas incorporating hydroxide are also possible.

Results

Synthesis and Composition. Tetraalkylammonium (TAA, alkyl = methyl, ethyl, propyl) containing manganese oxide gels were formed from the aging of colloidal precursors[23] at 85 °C in sealed polybottles. After gelation, the samples were either washed multiple times with distilled deionized water (DDW) or ion-exchanged with 0.1 M salt solutions (Na^+, Mg^{2+}, Cu^{2+}, Ni^{2+}, or La^{3+}), followed by washing. Drying in air or at 65 °C produced a dark brown powdery xerogel with a typical volume loss >50%. The resultant xerogels do not swell or reform a colloid when introduced to pure water; however, suspension in TAAOH solutions results in dissolution of the xerogel to form a reddish brown colloid visibly similar to the starting TAA manganese oxide colloids. If gels are not washed and are left to dry in air, they will lose water to produce a dark brown greasy solid.

Formulas and manganese oxidation state data for the TAA manganese oxide xerogels are presented in Table 1 and compared to a well-characterized alkali metal manganate, sodium birnessite (OL-1, Figure 1). Formulas were calculated from a combination of C,H,N analysis, Mn ICP-AES analysis, Mn average oxidation state titration, and TGA (for determination of adsorbed water). Formulas do vary from sample to sample as a function of aging time, temperature, and other factors but the reported values represent an average set of results. Generally, the TEA and TMA xerogels have similar formulas, except for water content, whereas the TPA xerogel has a smaller fraction of occluded cation and a lower manganese average oxidation state (3.5 for TPA vs 3.8 for TEA, TMA). X-ray absorption near-edge spectroscopy (XANES) data collected at the SSRL have confirmed the relatively low oxidation state of TPA, yielding a value of 3.53. Sodium birnessite, by comparison, has an intermediate oxidation state (3.57) and the largest ratio of occluded cation/manganese (4.0 Na/14 Mn).

Structural Analysis. X-ray diffraction data of as-prepared xerogels frequently exhibit a series of evenly spaced (in 2θ) reflections, and these are dependent on the identity of the TAA cation and post-treatment conditions of the xerogel (i.e., grinding). These reflections can be indexed to a layered birnessite-type phase (Figure 1, OL-1) with interlayer spacings similar to those observed when the corresponding colloid precursors or wet gels are cast onto glass slides.[23] There are, however, large differences in relative intensity between samples prepared by casting wet gels and those prepared from xerogels, as illustrated for TEA manganese oxide in Figure 2, a and b, respectively. Specifically, the (100) reflection at 2.4 Å (~35°) and the (111) at 1.4 Å (~60°, not shown) are increased in intensity relative to the (00*l*) reflections (3−25°) for the xerogel samples. Changes in peak positions, as well as relative intensities, are observed when the xerogels are subjected to mechanical stress (Figure 2c). For TEA manganese oxide xerogel, the (00*l*) peaks shift to lower *d* spacing (i.e., from 17.5 to 9.5 Å for the (001)) upon grinding, and the (100) and (110) reflections are less evident. This apparent collapse can be reversed. If the ground TEA manganese oxide xerogel is introduced to aqueous TEAOH, the resultant reddish brown colloid has a diffraction pattern identical to the starting TEA manganese oxide colloid (Figure 2d).

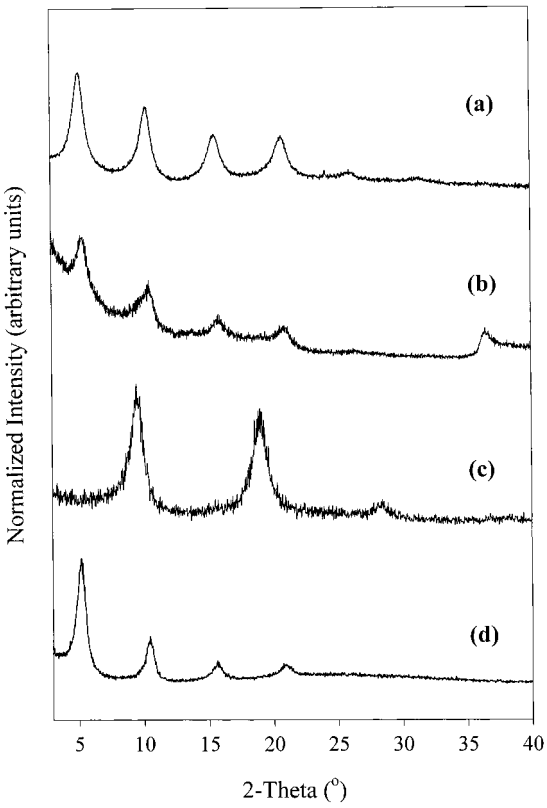

Figure 2. X-ray powder diffraction (XRD) patterns of (a) a wet TEA manganese oxide gel smeared on a plate and dried at room temperature, (b) a lightly crushed TEA manganese oxide xerogel, (c) a ground TEA manganese oxide xerogel, and (d) a colloid formed from dissolution of TEA manganese oxide xerogel in aqueous TEAOH.

Some samples are completely amorphous upon drying, even without any grinding or further processing. Therefore, EXAFS studies of an amorphous TPA manganese oxide xerogel were undertaken to probe the local structure. A plot of the real and imaginary part of the Fourier transformed EXAFS function, FT($\chi(k)$), is presented in Figure 3. The most prominent features in the FT(χ(k)) are peaks at ~1.5 Å and ~2.5 Å (not phase corrected), corresponding to Mn−O and Mn−Mn distances, and a third peak whose amplitude indicates the degree of collinearity along a chain of octahedra. The data can be fit to a monoclinic birnessite layered structure[30,31] with edge-sharing MnO_6 octahedra and a dihedral angle of 170° as shown in Figure 3. The fitting parameters and resultant bond distances are presented in Tables 2 and 3, respectively. SEM data are also consistent with a layered model (Figure 4). The platy morphology of the xerogels is very similar to that observed in birnessites.

Ion Exchange Properties. *Wet Gels*. Exchange properties of a TEA gel were probed using salt solutions containing Na^+, Mg^{2+}, Cu^{2+}, Ni^{2+}, or La^{3+}. The extent of the exchange was followed using chemical analysis, infrared spectroscopy, and XRD. For all the cations studied, the weight percent of carbon and nitrogen in exchanged samples are decreased by an order of magnitude relative to the TEA xerogel, consistent with the removal of the TEA cation in the exchange process. The ratio of exchange ion to manganese in the product is presented in Table 4 and compared with the ratio of TEA: Mn in an

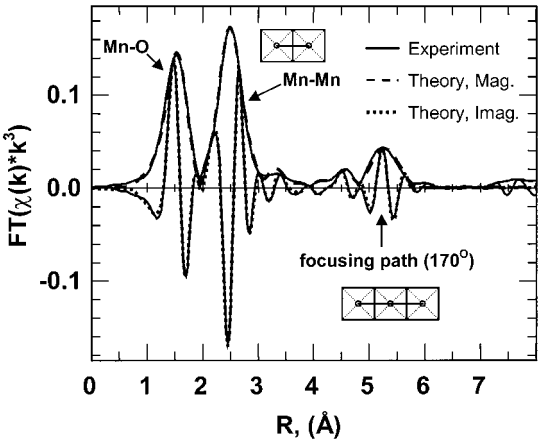

Figure 3. Fourier transformed experimental Mn K edge $\chi(k)k^3$ (real and imaginary part) functions and first derivative data for an amorphous TPA manganese oxide xerogel (not phase shift corrected). The prominent FT peaks are indicated and correspond to the Mn−O distance in an MnO_6 octahedron, the Mn−Mn distance between octahedra, and the focusing path corresponding to a near collinear (170°) arrangement of three octahedra. The fit of a birnessite type octahedral layered model to the experimental data is indicated ($R = 6.7\%$). Fit parameters and bond distance information are presented in Tables 2 and 3.

TABLE 2: EXAFS Refinement Parameters for Fitting Amorphous TPA Manganese Oxide Xerogel to an Octahedral Layered (OL) Structural Model

fit residual (R)	6.4%
fit range	1 Å to 5.8 Å
# independent parameters	42
# free running parameters	17
# single scattering paths	13
# multiple scattering paths	44
Debye temperature (O)	1027.61 K
Debye temperature (Mn)	561.468 K
energy shift (O)	0.549 eV
energy shift (Mn)	−2.75 eV
Mn−Mn−Mn angle[a]	170°
estimated error in *r*	∼0.03 Å

[a] To obtain good agreement between theoretical and experimental phases and amplitudes, collinear scattering paths at ∼5.5 Å were calculated with a displacement from collinearity of 10 degrees.

TABLE 3: Bond Distances (*r*), Standard Deviations (σ^2), and Coordination Numbers (CN) for Mn−O and Mn−Mn Pairs from an Octahedral Layered Model Fit to EXAFS Data for TPA Manganese Oxide Xerogel

pair	CN	distance *r* (Å)	σ^2
Mn−O	4	1.89	0.0031
Mn−O	2	1.91	0.0031
Mn−Mn	2	2.87	0.0044
Mn−Mn	4	2.86	0.0044
Mn−O	4	3.42	0.0038
Mn−O	2	3.54	0.0038
Mn−O	4	4.51	0.0038
Mn−O	4	4.52	0.0038
Mn−O	4	4.47	0.0038
Mn−Mn	4	4.95	0.0048
Mn−Mn	2	5.02	0.0048
Mn−Mn	2	5.69	0.0049
Mn−Mn	4	5.75	0.0049

analogous xerogel material. Additionally, charge normalized values have been computed by multiplying the A:Mn ratio by the charge of A (Table 4). The value for TEA manganese oxide xerogel (∼0.179) ideally represents the maximum cation-exchange capacity. Exchange with sodium or magnesium produce similar normalized A:Mn values, both less than that in the TEA manganese oxide xerogel. In contrast, Ni^{2+}, Cu^{2+}, and La^{3+} all exceed the ideal cation exchange capacity, with the greatest inclusion/adsorption occurring for Cu^{2+}.

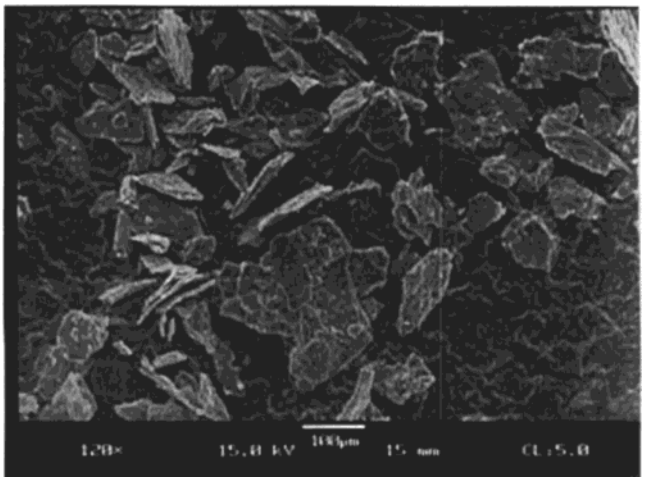

Figure 4. SEM micrograph of an amorphous TEA manganese oxide xerogel exhibiting the characteristic platy morphology of octahedral layered (OL) manganese oxide phases.

TABLE 4: Compositional and Structural Data for Ion-Exchanged TEA Manganese Oxide Gel. Charge Normalized Data Were Computed by Multiplying the Ratio A:Mn by the Charge of A; Subscript *t* Indicates a Turbostratic Asymmetric Lineshape, *b* Indicates a Broad Reflection. The Data Are Compared to an Average TEA Manganese Oxide Xerogel Sample

cation (A)	ratio A:Mn	charge normalized A:Mn	XRD reflections (Å) and indices (hexagonal subcell)
TEA	0.179	0.179	17.10 (001), 8.54 (002), 5.68 (003), 4.27 (004), 3.41 (005)2.4_t (100), 1.4_t (110)
Na^+	0.095	0.095	7.5_b (001), 2.4_t (100), 1.4_t (110)
Mg^{2+}	0.056	0.112	9.72 (001), 4.87 (002), 3.25 (003), 2.46_t (100), 1.42_t (110)
Ni^{2+}	0.213	0.417	2.4_t (100), 1.4_t (110)
Cu^{2+}	0.625	1.25	2.4_t (100), 1.4_t (110)
La^{3+}	0.213	0.625	2.4_t (100), 1.4_t (110)

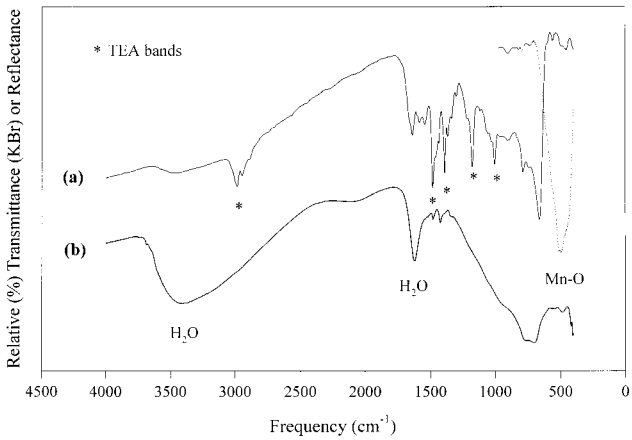

Figure 5. IR data for (a) a TEA manganese oxide xerogel, and (b) a xerogel produced from ion exchange with an aqueous sodium chloride solution. The transmission mode (solid lines) is more sensitive to the vibrations of the organic component and the reflectance mode (dotted lines) to Mn−O stretching.

Infrared analyses is a useful technique for determining the extent to which TAA cations can be exchanged out of the manganese oxide gel (Figure 5). TAA xerogels reveal a series of peaks between 1500 and 1000 cm^{-1} corresponding to C−H bending from CH_2/CH_3 groups (1500−1350 cm^{-1}) and C−N

stretching (1250−1000 cm^{-1}), and several peaks near 3000 cm^{-1} that are consistent with C−H stretching. However, upon exchange of the TEA manganese oxide gel with any of the five cations, all peaks due to TEA were absent, and no other peaks that could be attributed to other hydrocarbon phases were observed.

XRD was used to probe the effect of the exchange process on the structure of the manganese oxide xerogels. As indicated in Table 4, all the exchanged xerogels exhibit reflections at 2.4 and 1.4 Å corresponding to the (100) and (110) reflections in a layered birnessite structure. However, Na^+ and Mg^{2+} exchanged xerogels are unique in that they exhibit additional peaks that can be indexed as (00*l*) reflections. The sodium-exchanged sample has a weak reflection at 7.5 Å, producing a pattern identical to turbostratic sodium birnessite,[32] whereas the magnesium sample has several sharp reflections at 9.72, 4.87, and 3.25 Å as expected for Mg-buserite, a layer-expanded cousin to sodium birnessite. All the high *d* spacing peaks that are typical for TAA intercalated manganese oxide xerogel are absent after exchange, and there are no reflections corresponding to free salts of any of the exchange ions.

Xerogels. In contrast to wet gels, exchange of TEA manganese oxide xerogel with very concentrated, but pH neutral NaCl solutions results in an X-ray amorphous material. However, if the exchange is performed with a 0.1 M NaOH solution, the resulting solid has the same XRD pattern as Na-OL-1 prepared with high preferred orientation (7.26 Å, 3.61 Å)

Thermal Stability. The stability of the manganese oxide layered structure to thermal treatment was probed in the xerogel materials by XRD analysis of samples heated in air and TGA analysis in nitrogen. XRD patterns of TAA (TPA, TEA, TMA) xerogels heated in air at 100 °C are identical to materials dried at room temperature; however, upon heating to 200 °C in air, the material transforms to a single condensed phase, the spinel hausmannite (Mn_3O_4). In contrast, ion-exchanged gels retain peaks at 2.4 and 1.4 Å that are indicative of MnO_6 edge-sharing layers, even after heating at 200 °C, and no new peaks are observed. In a nitrogen atmosphere, as probed by TGA analysis, unexchanged materials exhibit abrupt weight losses with onset temperatures of 170 °C (TPA) and 190 °C (TEA, TMA) attributed to combustion of the TAA component. However, upon exchange with metal cations, no sharp weight losses are indicated below 400 °C in the nitrogen TGA.

Discussion

Structurally, tetraalkylammonium (TAA, alkyl = methyl, ethyl, propyl) manganese oxide gels are part of a class of well-known mineral phases (birnessites) that feature layers of edge-shared manganese oxide octahedra (OL, Figure 1) and share a number of properties with clays.[33] Synthetic birnessites (OLs) are conventionally prepared by precipitation methods and the interlamellar spacing is dependent upon interlayer cations. Exchange and swelling properties have been studied extensively, typically with metal cations,[34−36] although recently there have been reports of long chain alkylammonium and tetraalkylammonium cation incorporation into birnessites by synthetic templating, or exchange.[37−39] The resultant materials tend to be highly crystalline, reflecting the large, well-formed lamella often characteristic of host materials prepared by precipitation. In contrast, the sol−gel precursors are characterized by lamella with small diameters, as little as 40 Å.[23] Thus, it is not surprising that the degree of ordering is highly dependent upon treatment of the gel, or that gels are easy to exchange and can even be converted back to sols.

Wet gels that are spread onto a glass slide for XRD determinations yield a similar series of peaks to samples prepared from evaporation of colloids onto glass slides.[23] These systems are unique in that other manganese oxide gel preparations do not, to our knowledge, produce materials that demonstrate any crystallinity unless heated at high temperature.[13−22] Generally, only (00*l*) reflections are observed, and these can be modeled on layered phases with TAA cations and varying amounts of water between the lamella.[23] Typical interlayer spacings are noted in Table 1. As for the colloid precursor, the interlamellar dimension of the xerogel does not scale with the dimension of the TAA cation, instead it reflects a combination of the size and degree of hydration of the cation, with TEA having the greatest extent of hydration and thus the largest interlamellar spacing. Upon washing and air-drying, gentle crushing of the powder produces the same (00*l*) reflections (Figure 2b), but in considerably reduced intensity, plus two broad asymmetric peaks that can be indexed on the (100) and (110) reflections of the pseudo hexagonal OL structure. The asymmetric shape is a strong indication of turbostratic stacking in which the lamella are rotated with respect to each other along *c*, or are translated in the *ab* plane, and is another indication of poor crystallinity in xerogel materials.[32] The absence of the (100) and (110) in gels smeared onto glass slides (Figure 2a) is an indication of strong preferred orientation in these materials due to the preparation method. The TAA manganese oxide xerogel structures can easily be collapsed. If materials are ground with a mortar and pestle, XRD experiments indicate a reduced interlamellar spacing of 9.5 Å (Figure 2c). This is the normal interlamellar spacing for TMA, which has been suggested to have a structure in which cations are clustered at the edges of plates.[23] The shearing force inherent in the grinding may induce similar defect structures for TEA and TPA. Indeed, even when gently crushed, these peaks are evident superimposed over the peaks for the 17.5 Å phase of TEA manganese oxide xerogel (Figure 2b).

The structural integrity of xerogel phases varies considerably from sample to sample. In some cases, samples are completely amorphous. An EXAFS investigation was undertaken to see if the lack of long-range order in some samples is a reflection of disorder of the local structure around Mn. Extensive EXAFS treatment of manganese oxides in general,[40−42] as well as TAA colloids, and wet gels[30,31] has been previously undertaken. A similar model based on edge-sharing MnO_6 was found to give the best fit for our TEA manganese oxide xerogel system (Figure 3, Tables 2 and 3). In this respect, noncrystalline xerogels, while lacking long-range order, appear to be structurally very similar to colloids and gels. The model furthermore sheds some light on the distribution of Mn^{3+} and Mn^{4+} in the structure. Due to Jahn-Teller distortions, octahedra centered by Mn^{3+} are not collinear with $Mn^{4+}O_6$ octahedra, resulting in a pronounced effect on the intensity of the "focusing" peak at ~5.5 Å that corresponds to Mn−Mn−Mn distances. Thus, this peak can be fit with a model that takes into account variations of the Mn−Mn−Mn dihedral angle from 180°.[30,31] The obtained angle of 170° ± 3° is consistent with data from wet gels, and suggests that there may be some degree of ordering of Mn^{3+} in the structure along one direction leading to alternate $Mn^{3+}Mn^{4+}$-$Mn^{3+}Mn^{4+}$ ordering along one axis. The degree of ordering may well be a function of the average oxidation state. For the TPA manganese oxide xerogel it is near 3.5, consistent with 50:50 distribution of Mn^{3+} and Mn^{4+}.

With respect to Table 3, the Mn−O distances obtained are average distances of the "real" Mn−O distances (or pair of

distances) at the Mn^{3+} and Mn^{4+} sites. Since the number of free running parameters is limited in the EXAFS refinement, the "real" Mn−O distances in the layer structure cannot be resolved. The angular deviation from 180° that is estimated from the amplitude of the peak at 5.2 Å is evident in the Mn−Mn distances in Table 3. The first two Mn−Mn distances are identical, whereas the Mn−Mn distances at 5.69 and 5.75 Å are significantly different. Here, the distance pair 2.87 and 5.75 Å indicates a collinear arrangement, whereas the distance pair 2.86 and 5.69 Å indicates an angle of ∼170°. This is also in agreement with our structural models.[30]

The nanoscale diameters of the lamella in these samples and the poor degree of ordering suggest TAA manganese oxide gels may undergo rapid and quantitative ion exchange. As formed TAA manganese oxide gels have a TAA:Mn ratio of one, reflecting the ratio in the $TAAMnO_4$ precursor. However, only a small amount of these TAA cations are presumed to be associated with the negatively charged manganese oxide lattice. The high pH of the gels (>12), a consequence of the reaction between permanganate and 2-butanol,[23] suggests a large component of TAAOH, which is an amorphous, viscous oil for all the TAA cations studied. After washing to produce near-neutral gels, powdery brown xerogels can be obtained that have a maximum TAA:Mn ratio of 0.18 (TEA). This is considerably less than the cation capacity for a related sodium phase (Na-OL-1), which has Na:Mn = 0.29.[35] The smaller TAA component may be attributed to its larger size relative to Na^+ and/or weaker interactions with manganese oxide. TAA cations are known to be weaker structure directors than metal cations in zeolite synthesis, and these interactions are responsible for the ability to prepare stable, high Mn concentration manganese oxide colloidal solutions.[23] Thus, they have the potential for facile exchange and may be ideal precursors for the introduction of cocatalysts, mobile ions, or other species into manganese oxides.

Wet, unwashed gels undergo complete loss of all TAA cations with all of the exchange ions investigated (Na^+, Mg^{2+}, Ni^{2+}, Cu^{2+}, La^{3+}), as evidenced by chemical analysis (Table 4) and IR spectroscopy (Figure 5). This is not surprising as MnO_x helical gels were observed to undergo rapid uptake of K^+ with concomitant loss of TMA in potassium solutions, forming an OL structure (Figure 1).[24] In contrast, xerogels are much more difficult to exchange. Suspension of a TEA manganese oxide xerogel in 5.5 M NaCl results in an amorphous product instead of the expected 7 Å Na-OL-1. The exchangeability may be a strong function of the pH. Xerogels can essentially be redissolved to form colloidal manganese oxide by dispersion in aqueous TAAOH (Figure 2d). High hydroxide concentration is known to be important for dissolving and crystallizing manganese oxides (birnessite in particular)[43] and may facilitate delamination and exchange in the TAA manganese oxide xerogels. This may be the reason for facile exchange of unwashed (high pH) gels. Consistent with this analysis, xerogel exchanges performed with NaOH solutions lead to excellent exchange to yield highly crystalline 7 Å Na-OL-1.

The ideal exchange capacity is assessed by the quantity of interlamellar cations present in a xerogel (0.18 for TEA:Mn). For unwashed TEA manganese oxide gels, varying amounts of metal cations are taken up from solution, but all the TEA is removed. Unexpectedly, three cations had higher exchanges than theoretically possible based on the presumed TEA_xMnO_y formula. However, sodium and magnesium are well behaved with uptakes (normalized for charge) suggesting a little more than one-half the anionic charge is neutralized. Na^+ and Mg^{2+} exchange can be considered to be effectively topotactic, each yielding crystalline OL materials with expected interlayer spacings (∼7 and 10 Å, respectively, Table 4). The excessive uptakes of Ni^{2+}, La^{3+}, and especially Cu^{2+} do not appear to have influenced the characteristic lamellar structure of edge-sharing octahedra; the (100) and (110) of pseudohexagonal birnessite are preserved (Table 4). However, no (00*l*) reflections were present, suggesting that ordering of the lamella is destroyed by the exchanging cations. This observation, coupled with the fact that the theoretical exchange capacity has been exceeded, may indicate that strong association between these ions and the manganese oxide layers induces de-lamination. There is also the possibility, especially under basic conditions that favor dissolution and reprecipitation, that there may be substitution of cations for manganese within the lamella. Indeed, Cu^{2+} and Mg^{2+} are known to substitute for Mn in the framework of porous manganese oxides.[44] Furthermore, oxides or oxyhydroxides of all three salts could precipitate on the surface of the manganese oxide xerogel; however, there is no indication of any such phases from XRD analysis. The inclusion of metal ions also lends thermal stability to the lamellar structure of the xerogel. TAA xerogels transform into Mn_3O_4 (spinel) by 200 °C due to the combustion of the organic moiety; however, ion-exchanged samples still retain the characteristic (100) and (110) reflections of OL phases.

Conclusions

Tetraalkylammonium manganese oxide gels represent simple and versatile precursors for rapidly incorporating a variety of co-cations into manganese oxides. The key to successful exchange reactions is the incorporation of hydroxide into the reaction mixture, and this is most easily achieved by starting with wet, unwashed gels. Exchanged materials and native TAA gels are structurally similar, but show different degrees of ordering between the manganese oxide lamella. Exchange with Na^+ or Mg^{2+} produces ordered phases with interlayer distances of 7 and 10 Å, whereas Ni^{2+}, Cu^{2+}, and La^{3+} show no such ordering, appearing to be delaminated. The large quantities of Ni, Cu, and La found in exchanged materials further suggests strong surface adhesion and/or direct doping into the manganese oxide lamella, indicating an ion adsorption capacity much greater than predicted on the basis of lattice charge alone.

Acknowledgment. The support of the U.S. Department of Energy, Office of Basic Energy Sciences, Division of Chemical Sciences is gratefully acknowledged. EXAFS experiments were carried out at Stanford Synchrotron Radiation Laboratory, supported by U.S. DOE, Division of Chemical Sciences. The authors are grateful to Dr. Joe Wong for his assistance with the EXAFS measurements and to the Environmental Research Institute of the University of Connecticut for C,H, N, and ICP-AES metals analyses.

References and Notes

(1) Suib, S. L. *Chem. Innov.* **2000**, *30*, 27−33. Brock, S. L.; Duan, N.; Tian, Z. R.; Giraldo, O.; Zhou, H.; Suib, S. L. *Chem. Mater.* **1998**, *10*, 2619−2628.

(2) Manthiram, A.; Kim, J. *Chem. Mater.* **1998**, *10*, 2895−2909. Ibarra Palos, A.; Anne, M.; Strobel, P. *Solid State Ionics* **2001**, *138*, 203−212. Chen, R.; Zavalij, P. Y.; Whittingham, M. S.; Greedan, J. E.; Raju, N. P.; Bieringer, M. *J. Mater. Chem.* **1998**, *9*, 93−100.

(3) Shen, Y. F.; Zerger, R. P.; DeGuzman, R. N.; Suib, S. L.; McCurdy, L.; Potter, D. I.; O'Young, C. L. *Science* **1993**, *260*, 511−515.

(4) Tian, Z.-R.; Tong, W.; Wang, J.-Y.; Duan, N.-G.; Krishnan, V. V.; Suib, S. L. *Science* **1997**, *276*, 926−930.

(5) Ching, S.; Krukowska, K. S.; Suib, S. L. *Inorg. Chim. Acta* **1999**, *294*, 123−132.

(6) Luo, J.; Zhang, Q.; Suib, S. L. *Inorg. Chem.* **2000**, *39*, 741−747.

(7) Zhang, Q.; Luo, J.; Vileno, E.; Suib, S. L. *Chem. Mater.* **1997**, *9*, 2090−2095.
(8) Chen, R.; Zavilij, P.; Whittingham, M. S. *Chem. Mater.* **1996**, *8*, 1275−1280.
(9) Aronson, B. J.; Kinser, A. K.; Passerini, S.; Smyrl, W. H.; Stein, A. *Chem. Mater.* **1999**, *11*, 949−957.
(10) Rziha, T.; Gies, H.; Rius, J. *Eur. J. Mineral.* **1996**, *8*, 675−686.
(11) Feng, A.; Kanoh, H.; Miyai, Y.; Ooi, K. *Chem. Mater.* **1995**, *7*, 1226−1232.
(12) Brinker, C. J.; Scherer, G. W. *Sol−Gel Science*; Academic: San Diego, 1990.
(13) Witzemann, E. J. *J. Am. Chem. Soc.* **1915**, *37*, 1079−1091.
(14) Cuy, E. J. *J. Phys. Chem.* **1921**, *25*, 415.
(15) Ching, S.; Landrigan, J. A.; Jorgensen, M. L.; Duan, N.; Suib, S. L.; O'Young, C.-L. *Chem. Mater.* **1995**, *7*, 1604−1606.
(16) Ching, S.; Petrovay, D. J.; Jorgensen, M. L.; Suib, S. L. *Inorg. Chem.* **1997**, *36*, 883−890.
(17) Ching, S.; Roark, J. L.; Duan, N.; Suib, S. L. *Chem. Mater.* **1997**, *9*, 750−754.
(18) Duan, N.; Suib, S. L.; O'Young, C.-L. *J. Chem. Soc., Chem. Commun.* **1995**, 1367−1368.
(19) Bach, S.; Henry, M.; Baffier, N.; Livage, J. *J. Solid State Chem.* **1990**, *88*, 325−333.
(20) Bach, S.; Farcy, J.; Pereira-Ramos, J. P. *Solid State Ionics* **1998**, *110*, 193−198.
(21) Bach, S.; Pereira-Ramos, J. P.; Baffier, N.; Messina, R. *Electrochim. Acta* **1991**, *36*, 1595−1603.
(22) Bach, S.; Pereira-Ramos, J. P.; Baffier, N. *J. Solid State Chem.* **1995**, *120*, 70−73.
(23) Brock, S. L.; Sanabria, M.; Suib, S. L.; Urban, V.; Thiyagarajan, P.; Potter, D. I. *J. Phys. Chem. B* **1999**, *103*, 7416−7428.
(24) Giraldo, O.; Brock, S. L.; Marquez, M.; Suib, S. L.; Hillhouse, H.; Tsapatsis, M. *Nature* **2000**, *405*, 38−38. Giraldo, O.; Marquez, M.; Brock, S. L.; Suib, S. L. Hillhouse, H.; Tsapatsis, M. *J. Am. Chem. Soc*. **2000**, *122*, 9330−9331.
(25) Glover, D.; Schumm, B., Jr.; Kozowa, A. *Handbook of Manganese Dioxides, Battery Grade*; International Battery Materials, 1989; pp 25−32.
(26) Karpenko, V.; Kinney, J. H.; Kulkarni, S.; Neufeld, K.; Poppe, C.; Tirsell, K. G.; Wong, J.; Cerino, J.; Troxel, T.; Yang, J.; Hoyer, E.; Green, M.; Humpries, D.; Marks, S.; Plate, D. *Rev. Sci. Instrum.* **1989**, *60*, 1451.
(27) Ressler, T. *J. Synchr. Rad.* **1998**, *5*, 118.
(28) Koningsberger, D. C.; Prins, R. *X-ray Absorption Spectroscopy, Chemical Analysis*; Wiley: New York, 1988; Vol. 92.
(29) Rehr, J. J.; Booth, C. H.; Bridges, F.; Zabinsky, S. I. *Phys. Rev. B* **1994**, *49*, 12347.
(30) Ressler, T.; Brock, S. L.; Suib, S. L.; Wong, J. *J. Phys. Chem. B* **1999**, *103*, 6407−6420.
(31) Ressler, T.; Brock, S. L.; Wong, J.; Suib, S. L. *J. Synchr. Rad.* **1999**, *6*, 728−730.
(32) Holland, K. L.; Walker, J. R. *Clays Clay Minerals* **1996**, *44*, 744−748.
(33) Drits, V. A.; Silvester, E.; Gorshkov, A.; Manceau, A. *Am. Mineral.* **1997**, *82*, 946−961.
(34) Golden, D. C.; Dixon, J. B.; Chen, C. C. *Clays Clay Miner.* **1986**, *34*, 511−520.
(35) Golden, D. C.; Chen, C. C.; Dixon, J. B. *Clays. Clay Miner.* **1987**, *35*, 271−280.
(36) Luo, J.; Zhang, Q.; Huang, A.; Giraldo, O.; Suib, S. L. *Inorg. Chem.* **1999**, *38*, 6106−6113.
(37) Wong, S.-T.; Cheng, S. *Inorg. Chem.* **1992**, *31*, 1165−1172.
(38) Luo, J.; Suib, S. L. *Chem. Commun.* **1997**, *1997*, 1031−1032.
(39) Liu, Z.; Ooi, K.; Kanoh, H.; Tang, W.; Tomida, T. *Langmuir* **2000**, *16*, 4154−4164.
(40) Hwang, S.-J.; Park, H.-S.; Choy, J.-H.; Campet, G. *Chem. Mater.* **2000**, *12*, 1818−1826.
(41) Manceau, A.; Combes, J. M. *Phys. Chem. Minerals* **1988**, *15*, 283−295.
(42) Silvester, E.; Manceau, A.; Drits, V. A. *Am. Mineral.* **1997**, *82*, 962−978.
(43) Luo, J.; Huang, A.; Park, S. H.; Suib, S. L.; O'Young, C.-L. *Chem. Mater.* **1998**, *10*, 1561−1568.
(44) Nicolas-Tolentino, E.; Tian, Z. R.; Zhou, H.; Xia, G. G.; Suib, S. L. *Chem. Mater.* **1999**, *11*, 1733−1741.